

Carrier Transport in Cu-As-Se Amorphous Semiconductors

V.I.MIKLA¹, V.V.MIKLA²

¹ Institute for Solid State Physics and Chemistry, Uzhgorod National University, Uzhgorod, Voloshina 54, Ukraine

² Yazaki, Ukraine, Ltd

Corresponding author: mikla@univ.uzhgorod.ua

Abstract

Photocurrent transients in time-of-flight (TOF) regime have been investigated in order to obtain information on charge carrier transport in amorphous $\text{Cu}_x(\text{As}_2\text{Se}_3)_{1-x}$ films. Photocurrent transients shape in As_2Se_3 change with Cu addition. Drift mobility-temperature data indicate that hole transport in $\text{a-Cu}_x(\text{As}_2\text{Se}_3)_{1-x}$ alloys is controlled by a set of shallow traps at 0.40 eV above the valence band edge. On the basis of these observations, the density of gap states are considered from the point of view of multiple trapping.

Keywords: Chalcogenide; Cu-As-Se; Amorphous; Films; Transient photocurrent; Gap states

Received on

1. Introduction

Various fundamental properties (including structure) of elemental and binary chalcogenide glasses have been investigated extensively [1-16]. On the contrary, electronic properties of ternary chalcogenides were studied poorly [8-10]. Especially, this is true respectively for Cu-As-Se glasses. The latter are known to exhibit pronounced photoinduced phenomena [9,13,16].

Significant photodarkening effect in Cu-As-Se glasses and higher resolution in comparison with other materials of this group together with reversibility makes them especially attractive objects for optical data storage. In present, despite more than three decades of intensive study of this unique phenomenon, its origin remains unclear [17]. Reasonably, this essentially limits the possibility of materials fabrication with required properties, which determine the photoinduced changes of fundamental physical parameters. This is especially true for the case of Cu-As-Se glasses. There is no information in the literature, to our best knowledge, about the drift mobility in this ternary chalcogenides. The present article deals with charge carrier transport in $\text{a-Cu}_x(\text{As}_2\text{Se}_3)_{1-x}$ amorphous semiconductors.

2. Experimental

For the time-of flight experiments amorphous Cu-As-Se thin samples were used. These were prepared by flash thermal evaporation of bulk alloy Cu-As-Se from a molybdenum quasi-closed unit, using standard vacuum system (Model VES-5) with a base pressure $2-3 \times 10^{-6}$ Torr, as described previously [9]. The starting materials for pellets were from Cu-As-Se glasses prepared by usual melt-quenching technique. Substrates were glass for optical microscopic purposes with pre-deposited Au electrodes. The top electrodes were semitransparent films of evaporated gold. Sample thickness ranged from 3 to 5 μm , and was measured by a precision interference microscope (Model MII-4, accuracy not better than 0.05 μm).

The deposition rate was $\sim 1 \mu\text{m min}^{-1}$. Film thickness ranged from 3 to 5 μm . It is necessary to note that we have used a shutter protection system at initial and final stage for steady evaporation and deposition conditions to be established. We believe that the samples are relatively homogeneous as far as their charge transport properties are concerned. Some degree of sample inhomogeneity is unavoidable in the preparation of films unless one uses flash evaporation but this is the case for very thin films. In addition, some sample-to-sample variation in the exact compositions is also unavoidable. Because the hole lifetime is sensitive to the relative amounts of Cu and As_2Se_3 , we believe that the samples were relatively homogeneous across both the film surface and the film thickness. The total injected charge was keeping constant. The latter was obtained from integrating the time-of-flight photocurrent transient. To preclude a possible contribution of thickness variations of the sandwich structure into the resulting dispersion, different regions of the semitransparent Au contact were illuminated and the obtained photocurrent waveforms compared.

The details of the conventional TOF apparatus have been described in the extensive articles by Spear [18], Pfister [19] and Kasap [6]). In the present study a nitrogen laser was used to excite charge carriers. All experiments were single shot measurements in which the sample is pulsed from the laser and the corresponding photocurrent transient was captured on a single event storage oscilloscope. The oscilloscope (single event bandwidth 0.5 μs pulse duration, S8-14 Model) captured the whole TOF signal to enable integration of the photocurrent and hence the evaluation of the total injected charge. The spread in the photocurrent tail can be precisely measured.

Time-of-flight measurements were carried out using a short light pulse from a N₂ laser (wavelength 337 nm, pulse duration 8 ns). The duration of the pulsed light was sufficiently shorter than the carrier transit time. Between the measurements samples were short-circuited and dark rested to avoid the space charge effects that can cause a non-uniform field distribution within the bulk and a distorted TOF photocurrent signal. Prior to measurements the samples were rested for two weeks in darkness at room temperature. This procedure allowed us to perform TOF measurements on samples with stabilized structure and, accordingly, fundamental properties. It is well known fact that the build-up of trapped charge within the chalcogenide sample during repetitive cycles in TOF measurements is a serious problem. We have overcome the latter by using a single-shot mode of operation. There is no influence of the light pulse intensity on the TOF shape. In other words, the small signal approximation is valid. When examining the reproducibility of the TOF photocurrent shape, we observe the stability of this characteristic for successive light pulses. Undoubtedly, this means that no space charge is accumulated during the photoinjection and transit. When dispersion entirely masks the transit time cusp (usually determined by the position of the break in the current pulse), we define a statistical transit time from a double-logarithmic plot of the algebraically decaying current.

The measurements were performed on sandwich-cell configuration structures. Sandwich-cell consists of the chalcogenide film, evaporated on glass substrate equipped with previously deposited bottom electrode (SnO₂ or Au) and top semitransparent gold electrode. Between them were placed the chalcogenide film.

Time-of-flight experiments were performed using conventional measuring circuit.

3. Results and discussion

Fig. 1 summarizes the results of our TOF investigations. Only hole drift mobility can be measured in $\text{Cu}_x(\text{As}_2\text{Se}_3)_{1-x}$ by the technique outlined above, and at temperatures above 300 K a relatively well defined transit pulse is observed. The signal contained an initial decay in the form of a spike. We may consider three possibilities as origins causing the photocurrent decay in the pre-transit region. First, as the method of excitation involves the creation of a charge sheet near the top surface of the sample, it has been argued that the initial spike is due to movement of holes towards to the top surface. If this a case, then due to larger difference in electron and hole mobility in our samples, a large spike due to holes in electron response and a small spike due to electrons in hole response respectively should be observed. Furthermore, the duration of the spike should be inversely proportional to the appropriate mobility. Second, the current spike may be caused by a high-field region in the vicinity of the illuminated electrode. The initial current decay can be understood in terms of the relaxation of charge photoinjected into a distribution of localized states. A detailed analysis of transient signals in the Cu-As-Se system support this third explanation for the spike. For samples $\text{Cu}_x(\text{As}_2\text{Se}_3)_{1-x}$ with $x \geq 0.05$ at any fields applied in this experiment, a shoulder is always clearly revealed in the current decays followed by a long tail; the transit time is still discernible.

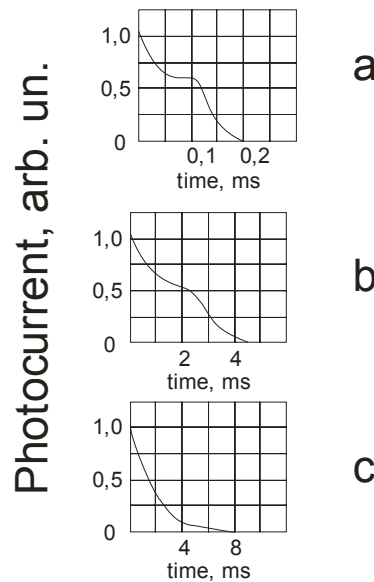


Fig. 1. Hole TOF photocurrent measured at $T = 325$ K (a), $T = 314$ K (b) and $T = 300$ K (c) in $\text{Cu}_x(\text{As}_2\text{Se}_3)_{1-x}$ (Cu concentration 5 at%) amorphous films at applied electric field – thickness ratio $0.25 \text{ V}\mu\text{m}^{-2}$. This and the following Figures illustrate the effects under consideration on the example of $\text{Cu}_x(\text{As}_2\text{Se}_3)_{1-x}$ at $x = 0.05$.

It should be also noted further characteristic features. First, and most encouragingly, TOF photocurrent shapes are very stable with respect to sample-to-sample variations. Second, for any sample we indeed observe true TOF signal and not any other (artifacts) – this fact is explained by experimental data for a relatively large range ($5 \times 10^4 - 4 \times 10^5 \text{ Vm}^{-1}$) of applied electric fields. The latter is illustrated in Fig. 3.

As expected, the transit time shortened with temperature. In analogy with the behavior observed in pure Se [20], hole traces for $\text{a-Cu}_x(\text{As}_2\text{Se}_3)_{1-x}$ show a progressive increase of transit time dispersion as the temperature is lowered (in our case from 325 K down to room temperature). It should be stressed on that as in the case of As_2Se_3 , it was not possible to detect any pulses associated with the transit of electrons. Only lifetime limited signals were observed for the case of photoinjected electrons. For these signals the transit time cannot be extracted by using even a double-logarithmic plotting. Transit pulses observed in $\text{a-Cu}_x(\text{As}_2\text{Se}_3)_{1-x}$ films may be characterized to first order as involving two power-law regimes:

$$I_1 \sim t^{-(1-\alpha_1)} \quad (1)$$

$$I_2 \sim t^{-(1+\alpha_2)} \quad (2)$$

The estimated from the signal slope of initial and final part, respectively, values of α_1 and α_2 are not equal to each other. As can be seen from the Fig. 1, the values of α_2 corresponding to the tail region of the TOF photocurrent transients, exhibit a much more rapid temperature dependence than those of α_1 . It becomes clear from the transients examination that universality of the pulse shape (predicted by a stochastic transport model [19]) with respect to temperature, applied electric field (Figs. 1-3) and sample thickness is not observed in our case. The qualitative observation is that for transients with relatively low magnitudes, which were observed at low T, the dispersion increased as the sample temperature is reduced. The same is also valid in respect to applied field, as well as for sample thickness.

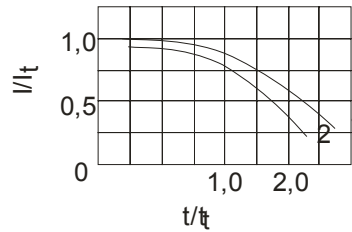


Fig. 2. Current traces at applied electric field $5.2 \text{ V } \mu\text{m}^{-1}$ (1) and $4.3 \text{ V } \mu\text{m}^{-1}$ (2). $T = 300 \text{ K}$.

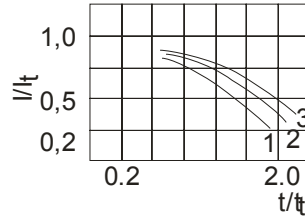


Fig. 3. Normalized photocurrent transients at $T = 348 \text{ K}$ (1), $T = 338 \text{ K}$ (2) and $T = 330 \text{ K}$.

The drift mobility value μ was estimated for well-defined transit time t_T according to the equation $\mu = d / E t_T$ [6,18,19], where d is the thickness of the sample and E is the applied electric field. Here we note that at room temperature, the transit time scales linearly with the sample thickness as expected (for details see, e.g. [21]) for transient transport with Gaussian dispersion. Drift mobility value is relatively independent of applied electric field, as actually observed in the experiments, and thermally activated with an activation energy $E_\mu \sim 0.4 \text{ eV}$.

In amorphous As_2Se_3 , the shape of the transient hole current even in dark-rested samples is typically dispersive and exhibits two distinct algebraic time dependences. In such a case, the transit time is identified by the intercept of the respective straight lines in the double-logarithmic plot [19].

Traditionally, charge carrier transport in pure and alloyed As_2Se_3 is considered within the framework of the multiple trapping model [6,21] and the density of state distribution in this material was determined from the temperature dependence of the drift mobility and from the post-transit photocurrent analysis. We can consider a short excitation pulse and infinitely strong absorption, so that only a thin sheet of carriers is produced in the sample near the top electrode. The injection levels are low, and we have neglected the effect of internal electric field due to the drifting carrier packet, and trap filling effects. In the present study, namely in $\text{a-Cu}_x(\text{As}_2\text{Se}_3)_{1-x}$, the hole transit time was measured in under the regime of equilibrium transport. This material has particularly long hole lifetimes so that deep trapping effects do not obscure the data.

The dominant feature of the density of state distribution in the lower half of mobility gap is the peak at ~ 0.4 eV above E_v introduced to explain the temperature dependence of drift mobility. The presence of this peak in all of our samples, and the relative stability of its value, imply that it may be connected with intrinsic defects in $a\text{-Cu}_x(\text{As}_2\text{Se}_3)_{1-x}$. Note that the peak mentioned is also present in host As_2Se_3 material.

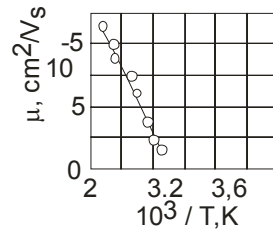


Fig. 4. Temperature dependence of drift mobility μ for Cu-As-Se amorphous films.

Reasonably that in our experiments we have observed and examined the photoinduced effects inherent for $a\text{-Cu}_x(\text{As}_2\text{Se}_3)_{1-x}$ amorphous layers. The influence of photodarkening on the hole TOF transient photocurrent illustrates Fig. 5.

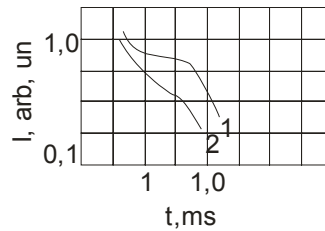


Fig. 5. TOF photocurrent in dark-rested (1) and pre-illuminated with band-gap light (2) amorphous films.

Just after irradiation a drastic change in transient photocurrent was observed. As can be seen from the same Figure, the dispersion of the transit pulse tends to increase with photodarkening. In fact, the initial (pre-transit) current slope increased whereas the final (post-transit) current slope decreased. The important result of this experiment is the observation that the hole drift mobility E_μ are the same before and after light exposure. A similar behavior of drift mobility we have observed on a number of other disordered chalcogenides. Here it is necessary to note that, for samples photodarkened to saturation, the $\log I$ versus $\log t$ plot yielded a straight line from which no transit time could be extracted. In such a case only a lifetime-limited signal is observed. Subsequent annealing restores the initial TOF photocurrent shape. Furthermore, the “insensitivity” of transit time to photodarkening means that the localized states that control the transport of charge carriers and determining the activation energy of drift mobility are not responsible for photoinduced changes in the shape of photocurrent transients. Substantial changes in deep states density, as we believe, are the reason for the observed photoinduced effects. At the same time, it should be emphasized that this explanation does not exclude other possibilities. The general observations in Fig. 5 agree with the effect of photoinduced changes on the photoelectronic properties, as reported by Abkowitz and Pai [22] and Mikla [5].

Drift mobility experiments may be affected by two kinds of space charge effect. First of all, it is the presence of deep centers in the mobility gap. These centers gradually accumulate charge with each drift pulse, especially near the surfaces of a specimen, which leads to a decreasing internal field. As a result the transient current decreases in magnitude. Secondly, at high photoinjection levels ($Q > CV$, where C is the sample capacitance and V is the applied field), space charge may be due to the drifting packet itself. In our case this latter can be excluded because of the small value of injected charge ($Q \leq 0.1CV$). It is obvious that band-gap light leads to the development of the pronounced variation in the space charge in the sample. The estimated amount of charge accumulated by deep traps during a ten-transit sequence increases 2 times at least at photodarkening and approaches approximately 10^{14} cm^{-3} . Consequently, shallow states which control charge transport and define the activation energy E_μ (for As_2Se_3 and $\text{Cu}_x(\text{As}_2\text{Se}_3)_{1-x}$ nearly 0.4 eV) of the mobility should not undergo photoinduced changes. At the same time it should be stressed that the observed change in the current transient (namely its increased dispersion and decreased magnitude) indicate photoinduced changes of deep states with $E_t > E_\mu$. Such behavior is probably related to enhanced carrier trapping by deep levels in photodarkened samples.

Finally, we will try to explain the effect of Cu alloying on transport properties of As_2Se_3 . The influence of Cu is complicate. On one hand, the addition of Cu substantially reduces the transit time, and, respectively, increases the drift mobility value. On the other, it seems to decrease the magnitude of the peak in the density of

states at 0.4 eV above E_v . A decrease in the concentration of these relatively shallow traps, in turn, causes an increase the drift mobility.

4. Concluding remarks

From time-of-flight study on amorphous $\text{Cu}_x(\text{As}_2\text{Se}_3)_{1-x}$ films the following conclusions have been obtained:

- (1) Only hole transport is observed; in contrast, for electron transport lifetime-limited photocurrent transients were inherent.
- (2) The dispersion of transit time increased with temperature lowering.
- (3) Drift mobility is thermally activated with $E_\mu \sim 0.4$ eV; as for the case of As_2Se_3 , the peak in the density of states located at E_μ above the valence band edge control the hole transport.
- (4) We have identified systematic photoinduced changes in hole transport with deep traps.

References

- [1] N.F.MOTT, and E.A.DAVIS, *Electronic Processes in Non-Crystalline Materials*, Clarendon. Oxford 1979.
- [2] M.POPESCU, *J. Non-Cryst. Solids* **352**, 887(2006).
- [3] V.KOLOBOV, *Photoinduced Metastability in Amorphous Semiconductors*, Wiley-VCH, Weinheim (2003).
- [4] J.SINGH, and K.SHIMAKAVA, *Advances in Amorphous Semiconductors*, Taylor and Francis, London (2003).
- [5] G.LUCOVSKY, and M.POPESCU, *Non-Crystalline Materials for Optoelectronics*, INOE Publishers, Bucharest (2004).
- [6] S.O.KASAP, in "Handbook of Imaging Materials" ed. by A.S.Diamond and D.S.Weiss, Marcel Dekker, Inc., New York, Second Addition, New York (2002).
- [6] S.NEOV, M.BAEVA, and M.NIKIFOROVA, *Physica Status Solidi (a)* **57**, 795(2006).
- [7] M.KITAO, H.AKAO, T.ISHIKAWA, and S.YAMADA, *Physica Status Solidi (a)* **64**, 493 (2006).
- [8] A.A.KIKINESHI, V.I.MIKLA, and D.G.SEMAK, *Ukranian J. Phys.* **23**, 63 (1978).
- [9] M.ITOH, *J. Non-Cryst. Solids* **210**, 178 (1997).
- [10] M.OHTO, and K.TANAKA, *J. Non-Cryst. Solids* **227**, 784 (1998).
- [11] K.S.LIANG, A.BIENENSTOCK, and C.W.BATES, *Phys. Rev.* **B10**, 1528 (1974).
- [12] J.Z.LIU, and P.C.TAYLOR, *Phys. Rev.* **B 41**, 3163 (1990).
- [13] Z.U.BORISOVA, *Glassy Semiconductors*, Plenum, New York, 1981.
- [14] A.A.VAIPOLIN, and E.A.PORAI-KOSHITS, *Sov. Phys. Solid State* **5** 497 (1963).
- [15] Y.ASAHARA, and T.IZUMITANI, *J. Non-Cryst. Solids* **16**, 407 (1974).
- [16] K.Tanaka, in "Encyclopedia of Materials", Elsevier Science Ltd., 2001 (p.1123).
- [17] W.E.SPEAR, *Proc. R. Soc. A* **420**, 201 (1988).
- [18] G.PFISTER, and H.SCHER, *Adv. Phys.* **27**, 747 (1978).
- [19] M.ABKOWITZ, and R.C.ENCK, *Phys. Rev.* **B 25**, 2567 (1982).
- [20] J.M.MARSHALL, *Rep. Progr. Phys.* **46**, 1235 (1983).
- [21] M.ABKOWITZ, and R.C.ENCK, *Phys. Rev.* **B 27**, 7402 (1983).